International Core Journal of Engineering Volume 5 Issue 10, 2019
ISSN: 2414-1895 DOI: 10.6919/ICJE.201909_5(10).0023

# Elastoplastic Analysis of Lattice Prism Tower under Impact Load

Yue Ma

Shanghai Offshore Engineering Research Institute, Shanghai Maritime University, Shanghai 201306, China

977862144@qq.com

## Abstract

**In this paper, based on the theory of vector structural mechanics, the impact analysis of lattice prism towers is carried out. The elastic-plastic changes of structural elements are clearly shown after the structure is subjected to impact loads. In addition, the transient dynamic analysis is carried out by the finite element software ANSYS to verify the results, which proves the superiority of this method. It provides a good numerical analysis method for the non-linear analysis of structures.**

## Keywords

**Vector Structural Mechanics, Lattice Structure, Impact, ANSYS.**

## 1. Introduction

With the vigorous development of large-scale machinery and equipment, the utilization rate of production equipment is getting higher and higher. Port equipment, as an important part of it, plays a vital role. Moreover, with the application of manufacturing technology and high-precision steel, crane boom is developing towards lightweight and latticed structure, latticed structure can reduce the quality of structure and wind load. Nevertheless, for this reason, for the application of high-precision steel, the latticed structure can reduce the quality of structure and wind load. The impact problem of crane boom structure still exists.

The results of impact are structural instability and collapse. To solve these problems, many experts have carried out in-depth research. Luo Weigang and Hei Xiaodan [1] used ABAQUS to study the influence of corner column failure on structural resistance to continuous collapse and the influence factors of residual structural dynamic response. Liu Zhao and Lu Zhiqiang [2] established failure model through LS-DYNA to judge fracture failure behavior. Yarimer, E. [3] analyzed the floor collapse caused by explosives through numerical model. Finally, the displacement time history of collapsed components was output. Wei Xiaolin [4] described the definition of building collapse mechanics and the characteristics of multi-body-discrete body dynamics, and carried out experimental verification through practical application. Collision impact problem can also be simulated by software. Xia Mingrui and Yin Chenbo [5] used the finite element analysis software Hypercrash to simulate the process of rigid leg collision of shipbuilding gantry crane crane lifts, and obtained the deformation mode and position stress. Bao Lei, Yin Chenbo, etc. [6] A rigid-flexible coupling virtual prototype model of shipbuilding gantry crane is established by using Pro/E, ANSYS and ADAMS software. Based on the analysis of structural elements by vector finite element method, Tung-Yueh Wu [7] uses vector finite element method to analyze the dynamic non-linearity of shell structure. Hudi, He Yong and Jin Weiliang [8] based on the principle of vector finite element, the structural motion response and the overall strength at each time point of Spar centralization process are analyzed in detail. Zhu Mingliang and Dong Shilin [9] based on MATLAB language and vector finite element method, track and simulate the whole process of cable and ring failure of suspended dome, and prove the accuracy of the analysis results by this method. H. -H. Lee, K. -W. Tseng, P. -

ISSN: 2414-1895 DOI: 10.6919/ICJE.201909_5(10).0023

Y. Chang [10] The dynamic response of a typical offshore formwork platform under wave force is analyzed by using plane frame element. Leige Xua, Mian Lin [11] Based on vector finite element method, the deformation and stress changes of beam-shell coupling structure under three ultimate states are studied.

Traditional finite element structural analysis can not fully show the changes before and after the impact process. In this paper, the vector finite element method is used to discretize the structure, get rid of the constraints brought by the stiffness matrix, and inverse the motion of the whole structure by the motion of particles, which greatly improves the calculation efficiency of the whole lattice prism.

## 2. Introduction of vector finite element theory

### 2.1 Basic content

Vector finite element method is proposed by Professor Ding Chengxian, which discretizes the bar element into several particles. Then, based on Newton's kinematics law, the internal force of the bar element can be obtained by force analysis of the particle and virtual work theory. This theory is different from the traditional finite element analysis. It does not integrate the whole stiffness matrix, does not have matrix singularity problem, and the process is greatly simplified. The non-linear analysis of component element brings forward new ideas.

The main body of vector finite element theory consists of three parts: point value description, path element and reverse motion. Point value description is to divide the bar into many particles and elements without mass, that is, to distribute the mass of the element to the particles, and to calculate and analyze the motion of the particles by using kinematics theory. The concept of path element is to consider the representation of continuum and discontinuity. When the structure collides, the description of the whole process is more complex. But the introduction of path element is to place each time period in each path element by discontinuous motion, and the deformation in one path element still follows the calculation of continuum, so that the whole process is discretized. Multiple units are analyzed in turn to show more clearly the change of structure after discontinuous movement. Reverse motion is to transform the initial problem of spatial bar element into the problem of pure deformation by translation or rotation, and then calculate it by traditional theory.

### 2.2 Internal force calculation of beam element

Take any bar element connecting point I and J, and the node of the element is 1 and 2. According to the basic hypothesis of material mechanics, the neutral axis of the element is straight, and the material and cross-sectional area are constant. In the pathway unit, $t_a \le t \le t_b$， The node displacement of the element is obtained from the positions of the connected space points I and J.$\left(\vec{u}_a^1, \beta_a^1\right)$及$\left(\vec{u}_a^2, \beta_a^2\right)$。

$$\begin{aligned}\left(\vec{u}_a^1, \beta_a^1\right) &= \left(\vec{x}_{Ia}, \theta_{Iza}\right) - \left(\vec{x}_{I0}, \theta_{Iz0}\right) \\ \left(\vec{u}_a^2, \beta_a^2\right) &= \left(\vec{x}_{Ia}, \theta_{Iza}\right) - \left(\vec{x}_{I0}, \theta_{Iz0}\right)\end{aligned} \tag{1}$$

When time t,the position of points is $\left(\vec{u}_a^1 + \vec{u}^1, \beta_a^1 + \beta^1\right)$ and $\left(\vec{u}_a^2 + \vec{u}^2, \beta_a^2 + \beta^2\right)$. During t to $t_a$ ,the displacement Vector of Bar Element is $\left(\vec{u}^1, \beta^1\right)$ and $\left(\vec{u}^2, \beta^2\right)$.

Setting up the principal axis coordinates of a group of elements $\left(\hat{x}_1, \hat{x}_2, \hat{x}_3\right)$， $\hat{x}_1$ axies coincide with meta-axis， whose direction is $\hat{e}_{n-1}^1$， and the other two directions are the principal axis of the cross section,then take $\hat{e}_{n-1}^1, \hat{e}_{n-1}^2, \hat{e}_{n-1}^3$ as the principal axis coordinate,and the transformation matrix between domain coordinates is

ISSN: 2414-1895 DOI: 10.6919/ICJE.201909_5(10).0023

$$\hat{x} = \begin{bmatrix} \hat{x}_1 \\ \hat{x}_2 \\ \hat{x}_3 \end{bmatrix} = \Omega_{n-1} x = \Omega_{n-1} \begin{bmatrix} x \\ y \\ z \end{bmatrix} \tag{2}$$

$$\Omega_{n-1} = \begin{bmatrix} \left(\hat{e}_{n-1}^1\right)^T \\ \left(\hat{e}_{n-1}^2\right)^T \\ \left(\hat{e}_{n-1}^3\right)^T \end{bmatrix} \tag{3}$$

The span of the member element and the rotation angle of the node in the time period are as follows

$$l_{n-1} = \left|x_{n-1}^2 - x_{n-1}^1\right|, l_n = \left|x_n^2 - x_n^1\right| \tag{4}$$

$$\beta^j = \beta_n^j - \beta_{n-1}^j,\ j = 1,2 \tag{5}$$

Then $\beta^j$ is converted to the principal axis coordinate component.

$$\hat{\beta}^j = \begin{bmatrix} \hat{\beta}_1^j \\ \hat{\beta}_2^j \\ \hat{\beta}_3^j \end{bmatrix} = \Omega_{n-1}\beta^j,\ j = 1,2 \tag{6}$$

Secondly, the direction change vector of the member axis is $\theta e_\theta$

$$\hat{e}_n^1 = \frac{1}{l_n}\left(x_n^2 - x_n^1\right) \tag{7}$$

$$\theta e_\theta = \frac{\hat{e}_{n-1}^1 \times \hat{e}_n^1}{\left|\hat{e}_{n-1}^1 \times \hat{e}_n^1\right|}, \theta = \sin^{-1}\left(\left|\hat{e}_{n-1}^1 \times \hat{e}_n^1\right|\right) \tag{8}$$

Then the deformation of the member element in this period is as follows

$$\begin{aligned} \hat{\theta}_{2t} &= \left(\theta e_\theta\right) \cdot \hat{e}_{n-1}^2 \\ \hat{\theta}_{3t} &= \left(\theta e_\theta\right) \cdot \hat{e}_{n-1}^3 \end{aligned} \tag{9}$$

The torsion angles of nodes 1 and 2 can be obtained $\hat{\varphi}_1^1, \hat{\varphi}_1^2$， and the bend angle of node 1,2 is $\hat{\varphi}_2^1, \hat{\varphi}_3^1$ 和 $\hat{\varphi}_2^2, \hat{\varphi}_3^2$

According to the basic formulas for calculating internal forces and bending moments of members,it caculates $\Delta\hat{f}_j, \Delta\hat{m}_j$

$$f = \left(\frac{EA}{l}\right)\Delta l\ , m = \left(\frac{GI}{l}\right)\Delta\varphi \tag{10}$$

According to the following formula

$$\hat{f}_n^{\,j} = \hat{f}_{n-1}^{\,j} + \Delta\hat{f}^{\,j} \tag{11}$$

$$\hat{m}_n^j = \hat{m}_{n-1}^j + \Delta\hat{m}^j,\ j = 1,2 \tag{12}$$

The principal axis coordinates of the nodes are obtained, and then the domain coordinates are converted to the initial position of the member element through forward movement, and the internal force vector is obtained.

$$f_n^{\,j} = R_t\left(\Omega_{n-1}^T \hat{f}_n^{\,j}\right) \tag{13}$$

ISSN: 2414-1895 DOI: 10.6919/ICJE.201909_5(10).0023

$$m_n^j = R_t\left(\Omega_{n-1}^T \hat{m}_n^j\right), j = 1,2 \tag{14}$$

# 3. Elastoplastic analysis

## 3.1 Example 1

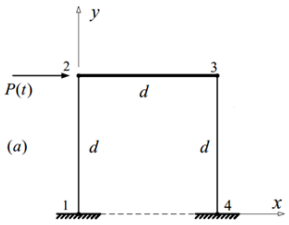


Fig. 1 Two-dimensional portal frame schematic diagram

The two-dimensional door frame consists of three members. The cross-sectional area of bar 12 and bar 34 is $0.125\,m^2$, the cross-sectional area of bar 23 is $0.25\,m^2$, Young's modulus is 1e6Pa, the external load is 5000N, the density is $50\,kg/m^3$, the analysis step is 1e-3s, and the termination time is 10s.

The impact load can be simplified as an external force applied in a very small time interval:

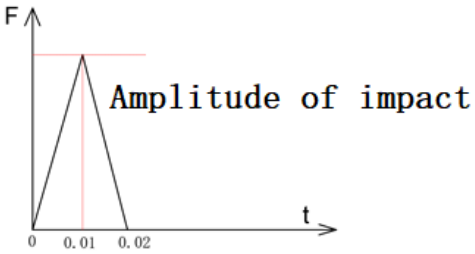


Figure 2 Impulse Load Applying Method

Elastic stage:

The following is analyzed by applying impact loads:

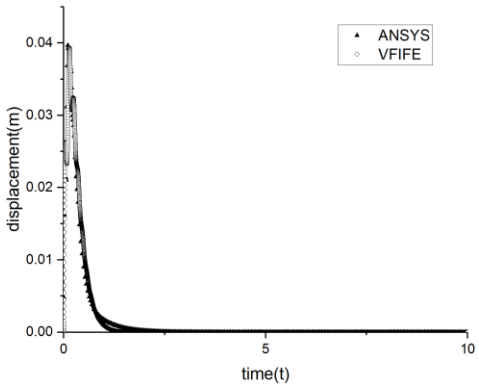


Figure 3. X-Directional Displacement-Time Variation of Node 2

From the figure, it can be seen that under the impact load and the influence of structural damping, the displacement of node 2 appears in the range of'hill'during the loading period. After unloading, the displacement of node 2 begins to decrease, and finally tends to 0.

Large Deformation (Plastic Stage):

ISSN: 2414-1895 DOI: 10.6919/ICJE.201909_5(10).0023

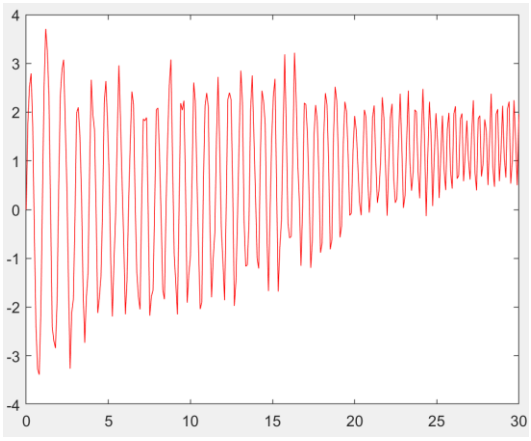


Figure 4 X-direction displacement (m) - time (s) change of node 2

In the large deformation stage, with the increase of the impact load, the plastic deformation of the structure will occur. The displacement of node 2 will not oscillate along the coordinate axis, but will begin to oscillate near a fixed deformation value, thus the deformation of the structure can be tracked.

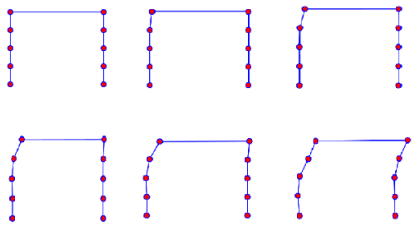

Fig. 5 Plastic Deformation Diagram of Structures

### 3.2 Example 2

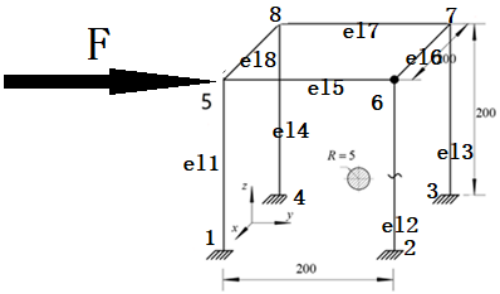


Figure 6. Three-dimensional portal frame schematic

Each rod is a round steel with a radius of 5 mm. Its elastic modulus E is 206 GPa and Poisson's ratio is 0.3. The horizontal force F is supported by impact load, structure and ground. The time step is 1 E-5 and the cut-off time is 2 s.

Elastic stage:

When the structure is subjected to impact load, the displacement of node 5 shows a trend of oscillation with time. Because the vector finite element method and finite element simulation have added appropriate damping, the displacement of the final node 5 of the whole structure gradually tends to zero. But in this case, the oscillation form of the vector finite element method has been reduced a lot, and the result converges faster. The image of node 5 is shown in the following figure. Show.

ISSN: 2414-1895 DOI: 10.6919/ICJE.201909_5(10).0023

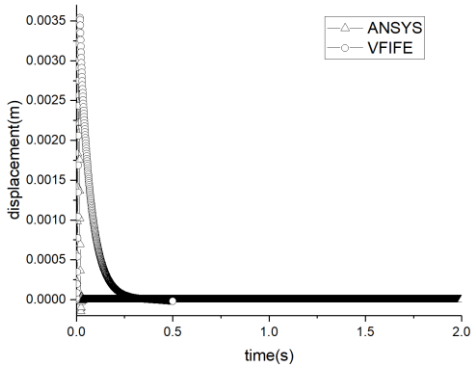


Figure 7. Y Directional Displacement-Time Variation at Node 5

As can be seen from the above figure, the stability of three-dimensional doorframe is much better than that of two-dimensional doorframe. When the impact load is unloaded and disappeared, the convergence speed of three-dimensional doorframe node is faster, which is also in the case of the same damping, and in the area where the load is applied, the image of two-dimensional doorframe still has some vibration, and the stability is relatively poor.

In conclusion, the results of two-dimensional and three-dimensional doorframes are within the normal error range, so the vector finite element analysis is relatively accurate, and the realization of the method theory is feasible.

Plastic analysis:

The ultimate bending moment is only related to material and section shape.

$$M_u = \sigma_s S \tag{15}$$

The ultimate bending moment is $M_u$， the yield strength of the material is $\sigma_s$ ,and the static moment of the section to the neutral axis is S.

The plastic state of the structure is judged by analyzing the form of plastic hinge, and the judgement statement is introduced. Four fixed fulcrums are excluded, and only the element where the moving point is located is analyzed.

Firstly, the impact load is increased to N, and then the position and time of plastic hinge are output by the vector finite element program.

Table 1 shows the sequence of plastic hinges (4 fixed joints are not considered)

| nodes | elements | time |
|---|---|---|
| 6 | 5 | 7.300E-04 |
| 7 | 6 | 7.300E-04 |
| 8 | 7 | 7.300E-04 |
| 5 | 8 | 7.300E-04 |

It can be seen from the table that plastic hinges appear at the locations of the four joints respectively after the impact load is applied. The bending moment caused by the deformation of the four joints has exceeded the limit value. Subsequently, with the unloading of the impact load, the structure has not changed significantly.A. Determine whether the internal force exceeds the critical value.

ISSN: 2414-1895 DOI: 10.6919/ICJE.201909_5(10).0023

## 4. Literature References

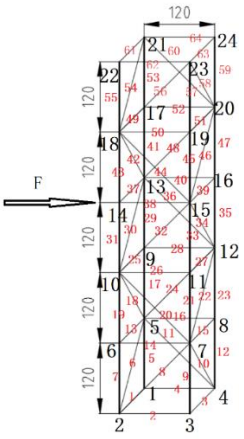


Figure 8 Structure of Lattice Prism Tower

The section of each element is $b \times h = 2 \times 10mm$: elastic modulus E is 206GPa, Poisson's ratio is 0.3, horizontal force F adopts impact load, structure and ground support, F = 5000N. Time step is 1e-5, cut-off time is 10s.

The following figure shows the displacement change of node 14s subjected to impact load during the 0-0.4s process (elastic-plastic stage)

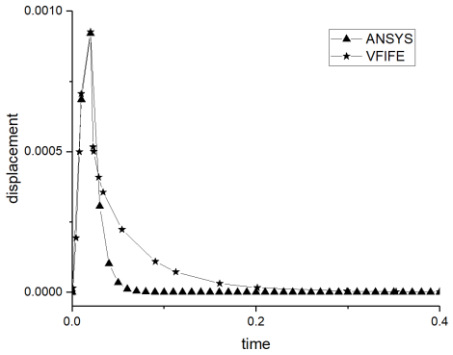


Fig. 9 shows the y-direction displacement-time variation of two analysis methods for node 14

The position and time of the plastic hinge are calculated by solving the ultimate bending moment and realizing the judgement statement. The state behavior of the structure is analyzed by combining the image.

When the load is increased to 5e7N, the plastic hinge appears. The first impact is around the point where the impact load is applied. Then the unit where the plastic hinge is located begins at No. 38 and gradually concentrates on the upper part of the element where the load is applied, while the lower part of the lattice prism tower does not appear the plastic hinge, so the structure enters the elastic-plastic stage.

Table 2 shows the order in which plastic hinges appear (4 fixed joints are not analyzed and are partially plastic hinges)

| nodes | elements | time |
|---|---|---|
| 14 | 38 | 1.720E-04 |
| 15 | 38 | 1.720E-04 |
| 16 | 39 | 1.720E-04 |
| 13 | 40 | 1.720E-04 |
| 17 | 41 | 1.720E-04 |

ISSN: 2414-1895 DOI: 10.6919/ICJE.201909_5(10).0023

| | | |
|---|---|---|
| 18 | 42 | 1.720E-04 |
| 18 | 43 | 1.720E-04 |
| 18 | 44 | 1.720E-04 |
| 19 | 45 | 1.720E-04 |
| 20 | 46 | 1.720E-04 |
| 20 | 47 | 1.720E-04 |
| 20 | 48 | 1.720E-04 |
| 18 | 49 | 1.720E-04 |

From the above part of the data, it can be seen that the number of plastic hinges in the unit where nodes 18 and 20 are located is on the high side, and the number of nodes 19 and 23 which are not listed in the data is also the same, which shows that from the top of the tower, the deformation of the second layer is obvious.

## 5. Conclusion

Based on the vector finite element theory, this paper analyses the elastic-plastic changes of plane and space beam structures under impact loads. The location and time of the plastic hinges are used to determine the shape of the structures. It plays an important role in the path tracing of space structures, and it is also a structure. Elastoplastic analysis provides a convenient method.

Because this method is applied relatively more in building structures and less in large-scale mechanical equipment (such as port crane), the calculation results of three-dimensional structures need to be verified by further experiments.

## References

[1] Luo Weigang, Hei Xiaodan, Liu Jibin. Dynamic Response Analysis of Continuous Collapse of RC Frame Structures Considering Floor Impact [J]. Journal of Architectural Science and Engineering, 2018, 35 (4): 113-119.
[2] Liu Zhao, Lu Zhiqiang, Wang Guangyao. Characterization and simulation prediction of fracture failure behavior of high strength steel and soft steel [J].Quarterly Journal of Mechanics, 2018,39(4): 829-836.
[3] Yarimer E. Compact Analysis Tool For Checking The Collapse Dynamics Of Buildings[J]. Réseaux, 2000,17(97):211-259.
[4] Wei Xiaolin. Development of blasting demolition technology and multi-body-discrete body dynamics [J]. Blasting, 2015 (1): 93-100.
[5] Ma Feng, Yin Chenbo, Xia Mingrui. Simulation analysis of collision end stop of shipbuilding gantry crane truck [J]. Machinery manufacturing and automation, 2014, 43 (4): 79-81.
[6] Baolei, Yin Chen-bo, Ma Feng. Collision simulation analysis of portal crane based on rigid-flexible coupling [J]. Modern Manufacturing Engineering, 2015 (11): 84-87.
[7] Wu, Tung-Yueh. Dynamic nonlinear analysis of shell structures using a vector form intrinsic finite element[J]. Engineering Structures, 2013, 56:2028-2040.
[8] Hudi, He Yong, Jin Weiliang. Spa centralized prediction and strength analysis based on vector finite element method [J]. Engineering Mechanics, 2012, 29 (8): 333-339.
[9] Zhu Mingliang, Dong Shilin. Failure analysis of suspended dome based on vector finite element method [J]. Journal of Zhejiang University (Engineering Edition), 2012, 46 (9): 1611-1618.
[10]Lee H H , Tseng K W , Chang P Y . The Application of Vector Form Intrinsic Finite Element Method to Template Offshore Structures[C]. Computational Mechanics:Proceedings of ISCM, 2007:298-298.
[11] Xu Leige, Lin Myanmar. Unevenness analysis of long-distance submarine pipeline based on vector finite element method [J]. Oil and gas storage and transportation, 2016, 35 (2): 208-214.
[12] Ding Chengxian, Duan Yuanfeng, Wu Dongyue. Vector Structural Mechanics [M]. Science Press, 2012.